The optical method based on gas injection overestimates leaf vulnerability to xylem embolism in three woody species

Francesco Petruzzellis[1], Azzurra Di Bonaventura[2], Enrico Tordoni[3], Martina Tomasella[1], Sara Natale[1,4], Patrizia Trifilò[5], Giuliana Tromba[6], Francesca Di Lillo[6], Lorenzo D'Amico[6,7], Giovanni Bacaro[1], Andrea Nardini[1]

[1]University of Trieste, Department of Life Sciences, Via L. Giorgieri 10, 34127, Trieste, Italy
[2]University of Udine, Department of Agricultural, Food, Environmental and Animal Sciences, Viale delle Scienze 206, 33100, Udine, Italy
[3]University of Tartu, Institute of Ecology and Earth Sciences, Department of Botany, J. Liivi 2, 50409 Tartu, Estonia
[4]University of Padova, Department of Biology, Via U. Bassi 58/B, 35121, Padova, Italy
[5]University of Messina, Department of Chemical, Biological, Pharmaceutical and Environmental Sciences, Viale Ferdinando Stagno d'Alcontres 31, 98166 Messina, Italy
[6]Elettra Sincrotrone Trieste, Area Science Park, 34149 Basovizza, Trieste, Italy
[7]University of Trieste, Department of Physics, Via A. Valerio 2, 34127, Trieste, Italy

Keywords:
Gas-injection; leaf hydraulics; micro-CT; optical method; xylem embolism.

Running head:
Gas injection overestimates optical vulnerability

For Peer Review

ABSTRACT

Plant hydraulic traits related to leaf drought tolerance like the water potential at turgor loss point (TLP) and the water potential inducing 50% loss of hydraulic conductance (P_{50}), are extremely useful to predict potential impacts of drought on plants. While novel techniques allowed the inclusion of TLP in studies targeting a large group of species, fast and reliable protocols to measure leaf P_{50} are still lacking. Recently, the optical method coupled with the gas-injection (GI) technique has been proposed as a possibility to speed up P_{50} estimation. Here, we present a comparison of leaf optical vulnerability curves (OVc) measured in three woody species, namely *Acer campestre* (Ac)*, Ostya carpinifolia* (Oc) and *Populus nigra* (Pn), based on bench dehydration (BD) or gas-injection (GI) of detached branches. For Pn, we also compared optical data with direct micro-CT imaging in both intact saplings and cut shoots subjected to BD. Based on the BD procedure, Ac, Oc and Pn had P_{50} values of -2.87, -2.47 and -2.11 MPa, respectively, while the GI procedure overestimated leaf vulnerability (2.68, 2.04 and 1.54 MPa for Ac, Oc and Pn, respectively). The overestimation was higher for Oc and Pn than for Ac, likely reflecting the species-specific vessel lengths. According to micro-CT observations performed on Pn, the leaf midrib showed none or very few embolized conduits at -1.2 MPa, consistent with the OVc obtained with the BD procedure but at odds with that derived on the basis of GI. Overall, our data suggest that coupling the optical method with GI might not be a reliable technique to quantify leaf hydraulic vulnerability, since it could be affected by the 'open-vessel' artefact. Accurate detection of xylem embolism in the leaf vein network should be based on BD, preferably of intact up-rooted plants.

For Peer Review

INTRODUCTION

Climate change is posing new challenges to both cultivated and wild plants, threatening crop productivity and ecosystem stability in different biomes (Lobell and Gourdji 2012, Forzieri et al. 2022). In particular, increased frequency and duration of drought events is concerning, considering that water availability constrains plant growth, reproduction and survival (Gardner 1965). In this view, plant functional traits related to drought tolerance have proved extremely useful to predict potential impacts of drought on plants (Cosme et al. 2017, Tordoni et al. 2022) and to assist breeding programs aimed at developing crop genotypes more adapted to harsher climatic conditions (Nardini et al. 2014, Sun et al. 2021).

Among the set of hydraulic traits relevant to assess plant performance under water limitation, two in particular stand out as reliable indicators of drought tolerance proving also to be suitable for modelling current and future plant distribution as a function of water availability. One of these is the turgor loss point (TLP) i.e. the leaf water potential corresponding to loss of cell turgor pressure (Tyree and Hammel 1972, Lenz et al. 2006). TLP sets the point at which stomata should close to prevent the risk of plasmolysis and cell damage, thus limiting the operating range of water potential for positive carbon gain (Rodriguez-Dominguez et al. 2016, Blackman 2018). The recent development of fast and reliable techniques for TLP estimation (Bartlett et al. 2012, Petruzzellis et al. 2019) has fostered the introduction of this parameter in ecological studies targeting large species' assemblages (Maréchaux et al. 2015, Tordoni et al. 2019, Petruzzellis et al. 2021), allowing. prediction of the impact of drought stress on plant performance (Zhu et al. 2018, Alvarez-Cansino et al. 2022, Petruzzellis et al. 2022) and modelling of current and future distribution of both woody and herbaceous species (Kunert et al. 2021, Tordoni et al. 2022).

The other trait strongly correlated with plant performance under drought is the vulnerability to xylem embolism (Tyree and Sperry 1989). Plants facing water shortage undergo a progressive drop of water potential and xylem pressure, which can be slowed down by stomatal closure but not completely prevented due to residual water loss at leaf and bark level

For Peer Review

(Wolfe 2020, Slot et al. 2021). When xylem pressure drops below species-specific critical values, a gas phase can be aspirated into water-filled conduits through inter-vessel pit membranes, leading to disruption of the continuity of water columns in the xylem network and hydraulic failure, potentially causing plant death (Nardini et al. 2013, McDowell et al. 2022). Plant vulnerability to xylem embolism is generally quantified in terms of P_{50}, i.e. the xylem pressure inducing 50% loss of xylem hydraulic conductivity (Venturas et al. 2017). In classical hydraulic studies, vulnerability to xylem embolism has been quantified at stem (Maherali and DeLucia 2000, Pockman and Sperry 2000) or leaf level (Neufeld et al. 1992, Nardini et al. 2001), and more rarely in roots (Sperry and Ikeda 1997, Kavanagh et al. 1999). The interest in measuring the vulnerability of leaf xylem steadily increased in recent years (Sack and Holbrook 2006, Nardini and Luglio 2014, Yan et al. 2020), considering that leaves are the terminal portion of the soil-to-atmosphere hydraulic pathway and are thus exposed to more severe water stress compared to stems and roots (Tyree and Ewers 1991). Moreover, leaves are the major photosynthetic organs in most plants, and thus any interruption of water delivery from leaf veins to mesophyll cells is expected to translate into an immediate reduction of photosynthetic rate and plant performance (Nardini et al. 2003, Hernandez-Santana et al. 2016, Bucci et al. 2019).

The validity of P_{50} as a proxy of plant performance under drought has been confirmed by several studies (Nardini et al. 2013, Oliveira et al. 2019, Petruzzellis et al. 2022), but its large-scale applicability is curbed by the time-consuming nature of classical hydraulic techniques, coupled with concerns for possible artefacts arising from such measurements (Wheeler et al. 2013, Trifilò et al. 2014). The introduction of low-cost optical techniques (Brodribb et al. 2016) has allowed direct observation of embolism formation and progression in the leaf xylem (Cardoso et al. 2022), providing an apparently artefact-free method for quantification of P_{50}. Still, a major disadvantage of optical measurements is that they rely on bench-dehydration of intact plants or excised branches to induce a progressive drop of leaf water potential and xylem pressure, leading to embolism formation in the leaf veins (Brodribb et al. 2016). This experimental procedure allows to measure leaf vulnerability curves, but it takes from a few

For Peer Review

hours for some very vulnerable species, to several days for leaves of drought-tolerant plants (Skelton et al. 2018, Blackman et al. 2019), thus preventing a widespread use of this technique.

A recent study has proposed a modification of the original optical technique, based on induction of leaf xylem embolism via injection of gas at progressively increasing pressure from the cut base of the petiole (Hochberg et al. 2019), allowing generation of a complete optical vulnerability curve within only 1 h. This experimental approach is based on the air-seeding hypothesis, stating that the gas phase leading to embolism enters a functional water-filled xylem conduit through inter-vessel pits, when the pressure difference between the liquid phase inside the conduits and a gas phase in an adjacent compartment surpasses a critical threshold (Tyree and Sperry 1989), likely set by the dimensions and the tortuosity of the pit membrane pores (Choat et al. 2003, Levionnois et al. 2022).

Experiments comparing embolism level in stems caused by dehydration-induced low xylem water pressure versus application of high gas-pressure from the outside (Cochard et al. 1992), have tested the validity of the air-seeding hypothesis but also paved the way for a new method for fast generation of hydraulic vulnerability curves (Salleo et al. 1992). Adapting this technique to the optical method for generation of leaf vulnerability curves would certainly boost the adoption of leaf P_{50} in ecosystem-scale studies (Skelton et al. 2019), provided this approach can generate reliable values. The use of positive pressures to quantify stem vulnerability to xylem embolism has been shown to produce substantial artefacts and over-estimation of P_{50} (i.e. values less negative than expected) in several species (Ennajeh et al. 2011a, Torres-Ruiz et al. 2014, Chen et al. 2021), claiming for further cautions in its application (Ennajeh et al. 2011b, Martin-StPaul et al. 2014). Hochberg et al. (2019) tested this method on leaves of two species (*Quercus rubra* L. and *Vitis vinifera* L.), comparing optical vulnerability curves generated via the classical bench dehydration and the gas-injection technique. While for *Q. rubra* the two methods yielded comparable results, in grapevine the gas-injection method over-estimated leaf hydraulic vulnerability by about 0.4

For Peer Review

MPa, highlighting the need for more empirical tests on different species before adopting the new method as a standard for fast generation of leaf optical vulnerability curves.

In this study, we present a comparison of leaf optical vulnerability curves generated for three woody species (*Acer campestre* L., *Ostrya carpinifolia* Scop., *Populus nigra* L.), based on bench dehydration or gas-injection of detached branches. For one species (*P. nigra*), we further compared optical data with direct micro-CT imaging of the functional status of leaf xylem conduits in both intact saplings and cut shoots subjected to bench dehydration. We specifically aimed at testing the general validity of the gas-injection technique for fast generation of leaf optical vulnerability curves, or highlighting possible pitfalls preventing recommendation of the technique for large-scale ecological studies.

MATERIALS AND METHODS

Plant material and experimental procedure

Experiments were performed in summer 2020 on three woody species: *A. campestre* (Ac), *O. carpinifolia* (Oc) and *P. nigra* (Pn). Plant material was harvested from adult trees (one tree per species) growing in the Botanical Garden of the University of Trieste (Italy). Branches were detached from the main trunk and the cut section was immediately put under water. Additional cuts were made underwater to remove any eventual emboli induced by the initial cut. Branches were > 1 m long to minimize the risk of experimental artefacts due to spurious embolism formation in open vessels (Torres-Ruiz et al. 2014, Petruzzellis et al. 2020), as mean vessel length in the studied species is 3, 5, and 20 cm for Ac, Oc and Pn, respectively (Nardini et al. 2012, Petruzzellis et al. 2020). Branches were then transferred to the laboratory, covered with a black plastic bag and rehydrated overnight. Optical vulnerability curves (OVc, Brodribb et al. 2016) were measured in each species following two different dehydration procedures, i.e bench dehydration (BD) and gas injection (GI). For the bench dehydration procedure, branches were dehydrated under laboratory conditions and allowed

For Peer Review

to reach different leaf water potential (Ψ_{leaf}) to induce the formation of different levels of embolism in the leaf vein xylem. In contrast, gas-injection was applied to fully hydrated branches by forcing gas entry in the leaf xylem under known pressure values. The basic principle of this technique is that the positive pressure needed to force a gas phase inside a water-filled conduit equals the xylem tension needed to aspire the gas phase under water stress, except for the sign which is opposite (Cochard et al. 1992, Martin-StPaul et al. 2014). Thanks to the OV method, embolism formation can be detected as a localized colour change, which corresponds to a change in light transmission through the xylem.

Bench dehydration (BD) procedure

Before starting measurements, Ψ_{leaf} was measured on one leaf for each branch using a Scholander pressure chamber (1505D, PMS Instrument Company, Albany, USA). Branches with $\Psi_{leaf} \geq -0.2$ MPa were considered as fully hydrated and suitable for OV measurements, carried out following the method described in Petruzzellis et al. (2020) with some modifications. According to vessel length, twigs of 10-15 cm were used for Ac and Oc (maximum vessel length of terminal twigs was 3 and 5 cm, respectively), while twigs of 30 cm were used for Pn (vessel length of terminal twigs was 20 cm). Then, one leaf without any damage symptoms was selected from each twig and was tightly attached with transparent tape to a cardboard mask, used to highlight a selected leaf area and prevent any potential light disturbance caused by the LED strip (1200 lumen). The leaf was secured to a Plexiglas panel with the adaxial surface facing the portion of the panel with a rectangular hole. This set up allowed to reduce sample's movement and shrinking during dehydration, while ensuring leaf-to-air gas exchange through the rectangular hole. A piece of grid paper was added on the Plexiglas panel to set the scale for the following image analysis. To avoid light scattering, the Plexiglas was placed towards the LED strip and the abaxial leaf surface towards the smartphone camera (models used: Asus Zenfone 4 Max and Nokia Lumia 1320). Twigs were let dehydrating in the laboratory at a room temperature and relative humidity of 25°C and 40%, respectively, for different time intervals, from a minimum of 30 min to a maximum of 24

For Peer Review

h, and Ψ_{leaf} was measured on each scanned leaf at the end of each dehydration time. A total of 16, 19 and 27 leaves were measured for Ac, Oc and Pn respectively.

Gas-injection (GI) procedure

Before starting measurements, Ψ_{leaf} was measured as described for the BD procedure. For each species, twigs with similar length of those used for BD procedure were detached from the stem and inserted in a series of gaskets: 1) PP cap; 2) sealing sleeve; 3) one 4 mm size and two 2 mm inner diameter rubber O-rings (Cole-Parmer Instrument Company). Then, they were firmly screwed on a PTFE cone (Cole-Parmer Instrument Company) connected to the Scholander pressure chamber through a high-pressure capillary tube. The Scholander pressure was connected to a tank filled with dry N_2. For each twig, one leaf without any damage symptom was mounted on the OV-set up as described for the BD procedure. Each twig was then subjected to a gradual pressure (P_{inj}) increase. Starting from a value of 0.5 MPa, pressure was increased by 0.3/0.5 MPa every 3 min, up to a maximum of ~5.0 MPa. In total, 9, 16 and 28 leaves were scanned for Ac, Pn and Oc, respectively.

Image capture and analysis

Each smartphone was connected to a personal computer and the screen was mirrored using the app Vysor (v 2.2.2) for Android OS and ProjectMyScreenApp (v 1.2) for Microsoft OS (Petruzzellis et al. 2020). By using AutoIT software (v 3.3.14.3), the mouse was set to automatically click on the “take pictures” command of the camera (Petruzzellis et al., 2020). To obtain higher quality images, manual mode of the camera was used to manipulate some settings like camera light sensitivity (ISO), white balance (WB) and exposure value (EV). For Android OS, the following options were applied: ISO=400, WB=2500 and EV=+0.3 for warm light LED; ISO= 800, WB=4000 and EV=0 for cold light LED. For Microsoft OS: ISO=400, WB=4000 and EV=0 for cold light LED. Images were taken every 30 and 90 seconds for the gas-injection and bench dehydration procedures respectively, and image sequences were processed in ImageJ (Schneider et al. 2012) with the “OSOV toolbox” plugin following the

For Peer Review

procedure described in http://www.opensourceov.org. To estimate the embolized vein length per unit area (VLA_{emb}), the cumulative length of embolized veins and leaf total area were measured, and VLA_{emb} was measured as:

VLA_{emb} = Cumulative length of embolized veins / Leaf area [mm mm^{-2}] (1)

For BD, one VLA_{emb} value was calculated for each scanned leaf and OV curves were calculated coupling VLA_{emb} and Ψ_{leaf} values measured at the end of the experiment. Conversely, for the gas-injection procedure, VLA_{emb} values were calculated for each value of applied pressure, and a complete OV curve was generated for each sample.

Statistical analysis

P_{12}, P_{50} and P_{88} values and associated 95% confidence intervals (CIs) were calculated for each dehydration procedure (i.e. BD and GI) and for each species using the *fitplc* R package (Duursma and Choat 2017) and R 4.2.1 (R Core Team, 2020). Specifically, OV curves were fitted using a Weibull model (Ogle et al. 2009), following Duursma and Choat (2017), and 95% CIs were calculated through the bootstrap procedure (n = 1000). Moreover, for the GI dehydration procedure, sample ID was set as a random effect in the Weibull model. For sake of comparison, we reported P_{12}, P_{50} and P_{88} derived from both BD and GI OV curves as negative values. Differences between P_{12}, P_{50} and P_{88} values calculated using BD and GI OV curves were considered statistically different when 95% CIs did not overlap.

Previous studies quantified optical embolism by calculating the ratio of the of embolized area at any Ψ_{leaf} and the total embolized xylem area after complete dehydration (as % of xylem embolized area; Brodribb et al. 2016; Cardoso et al. 2020; Avila et al. 2021). These studies measured Ψ_{leaf} continuously using a leaf psychrometer, but on a different leaf than the one attached to the "optical apparatus", assuming water potential equilibrium and similar embolization pattern in adjacent leaves. For BD, we measured Ψ_{leaf} using a pressure chamber on the same leaf used for optical embolism detection. Consequently, for each sample, we

For Peer Review

stopped the image acquisition at different times, detached the leaf from the "optical apparatus" and measured Ψ_{leaf}, preventing us to calculate the total embolized xylem area for each sample. For this reason, we calculated VLA_{emb} following Petruzzellis et al. (2020). On the other hand, the GI procedure allowed us to measure both Ψ_{leaf} and the applied pressure on the same leaf. In this light, for the GI procedure we also calculated the optical embolism as the % of embolized xylem area and compared P_{12}, P_{50} and P_{88} values with those obtained using VLA_{emb}. Differences between P_{12}, P_{50} and P_{88} values calculated using VLA_{emb} and the % of xylem embolized area approaches were considered statistically different when 95% CIs did not overlap.

Additionally, for each species we calculated the difference between P_{50} (obtained using VLA_{emb} as optical embolism measurement) values obtained through BD and GI procedure as follow:

$$\Delta P50 = |BD\ P_{50}| - |GI\ P_{50}| \quad (2)$$

where $|BD\ P_{50}|$ and $|GI\ P_{50}|$ correspond to P_{50} absolute values obtained through the BD and GI procedures, respectively.

Measurements of Leaf Vein Length per Unit Area

To compare VLA_{emb} to the total VLA, VLA of major (VLA_{maj}) and minor (VLA_{min}) veins were measured on 5 leaves for each species as:

$$VLA = \text{Vein Length} / \text{Leaf sample area}\ [\text{mm mm}^{-2}] \quad (2)$$

For major vein analysis, leaves were scanned with a desktop scanner and VLA_{maj} was measured using PhenoVein software (Bühler et al. 2015). VLA_{min} was measured following Petruzzellis et al. (2021). Specifically, small leaf portions (~2 cm^2) were cut from 5 leaves per species and treated in 1 M NaOH solution for 72 h. Samples were further bleached with a NaClO 5% solution, dehydrated in a sequence of ethanol solutions at increasing concentrations (25%, 50%, 75% and 100%) and immersed in an ethanol solution of toluidine

For Peer Review

blue (2%) overnight. Samples were then treated in a series of ethanol solutions at decreasing concentrations. Before preparing microscopic slides of the samples, leaf hairs were carefully removed with a small brush. Images were then captured using the Zeiss AxioPlan fluorescence microscope equipped with a digital camera (model: CS505CU – Kiralux 5.0 MP Color CMOS Camera, Thorlabs) and VLA_{min} was measured with PhenoVein software.

Phase contrast micro-CT observations

Despite the advantages of measuring OVc using the GI procedure (e.g. low number of samples needed, fast measurements), some studies have reported that GI could produce very high-threshold xylem pressure for embolism (i.e., low P_{50} values) compared with what is expected by using the standard BD procedure (Martin-StPaul et al. 2014). However, even the BD procedure, when applied to detached twigs, could be affected by an "open vessel artefact" (Lamarque et al. 2018). In this light, we performed micro-CT scans on Pn leaves at the SYRMEP beamline of the Elettra Synchrotron light source (Trieste, Italy) to validate the results obtained through the OVc. Specifically, micro-CT observations were performed using the propagation-based phase contrast modality (Fitzgerald 2000) on leaves attached to both intact individuals and cut shoots from 2-years-old Pn plants (saplings provided by a Regional Forest Service nursery). For each sample, Ψ_{leaf} was measured on one leaf using a Scholander pressure chamber (1505D, PMS Instrument Company, Albany, USA). As for the other procedures previously described, samples with a $\Psi_{leaf} \geq -0.2$ MPa were considered as fully hydrated and suitable for micro-CT measurements. To visualize the degree of embolization of the xylem vessels of the midrib at different Ψ_{leaf}, cut branches or entire plants were left dehydrating for different time intervals. Then, the shoot/plant was tightly attached to a wooden support to prevent any movement during sample rotation. For each shoot/plant, one leaf still connected to the stem and without any damage symptoms was selected, sealed in transparent tape and attached to the wood support with parafilm. The wooden support was placed within the sample holder and the scanning portion (~ 5 mm) of the midrib was aligned with the beam. Two filters (1 mm of aluminium and 1 mm of silicon) were used to obtain an

For Peer Review

average X-ray source energy of 22 keV. Exposure time was set at 100 ms, at an angular step of 0.5° s^{-1}, and the adopted sample-to-detector distance was 12 cm. During the 180° rotation of the sample, a total of 1800 projections were acquired. In total, 2048 slices per sample with a pixel resolution of 1 μm, were reconstructed using the SYRMEP TomoProject software (Brun et al. 2015). Ψ_{leaf} was measured immediately after image acquisition as described above. Images were acquired at Ψ_{leaf} ranges of -0.90/-0.95, -1.10/-1.20 and -1.60/-1.70 MPa (n = 2 for each Ψ range and group). These values were in the range of Ψ_{leaf} inducing either no embolism (-0.90/-0.95 MPa) or some initial embolism in the BD procedure (-1.10/-1.20 MPa) and leading to 50% embolism in the GI procedure (-1.60/-1.70 MPa).

RESULTS

OV curves

In the BD procedure, leaves were dehydrated over different time intervals to reach a final Ψ_{leaf} of about -4 MPa in Oc and -5 MPa in Ac and Pn. During dehydration, the first embolism events were detected in the major veins at -1, -1.5 and -1.8 MPa in Pn, Ac and Oc, respectively (Fig. 1). These events occurred in the midrib and propagated in minor veins as Ψ_{leaf} progressively became more negative (Fig. 1). In the GI procedure, gas was injected in leaf samples at a maximum P_{inj} of about 4 MPa in Ac e Pn and 5 MPa in Oc. The spatial pattern of gas propagation was similar to that observed in the BD procedure (Fig. 1), with embolism events initially occurring in the major veins, in particular in the midrib, and then propagating to the minor veins. However, the first embolism events generally occurred at relatively lower P_{inj} values (0.5 and 1.3 MPa, Fig. 1), compared with the BD procedure.

P_{12}, P_{50} and P_{88} values and associated 95% C.I.s are reported in Tab.1. P_{12} values calculated with BD and GI procedures differed in Oc and Pn, as the 95% CIs did not overlap in these species (Tab. 1). Based on the BD procedure, Ac, Oc and Pn had P_{50} values corresponding to -2.87, -2.47 and -2.11 MPa, respectively. On the other hand, using the GI procedure, P_{50}

For Peer Review

values were -2.68, -2.04 and -1.54 MPa in Ac, Oc and Pn, respectively. P_{50} values measured with the two dehydration procedures did not differ in Ac and Oc, as indicated by overlapping 95% CIs (Tab.1 and Fig. 2). On the contrary, P_{50} measured using the GI procedure was significantly lower than in BD for Pn (1.54 vs -2.11 MPa, Tab. 1 and Fig. 2). P_{88} values obtained with the BD procedure did not differ from those obtained with GI, as suggested by the non-overlapping 95% CIs (Tab. 1). A complete summary of the Weibull models run to calculate P_{12}, P_{50} and P_{88} values is available in Tab. S1. In general, P_{12} and P_{50} values calculated using the GI procedure tended to be higher than those calculated with BD. Considering P_{50}, this discrepancy was higher in Pn (ΔP_{50} = 0.57 MPa) and lower in Ac (ΔP_{50} = 0.19 MPa) and Oc (ΔP_{50} = 0.43 MPa), reflecting species-specific vessel lengths (Fig. 3).

Regarding possible differences arising from different optical embolism quantification, we detected similar P_{12} and P_{50} values obtained using VLA_{emb} and the % of embolized xylem area, except for P_{50}, which was lower using the VLA_{emb} approach in Pn (Tab. S2). On the contrary, significant lower P_{88} values were obtained using the VLA_{emb} approach in all the three species (Tab. S2). A complete summary of the Weibull models run for this analysis is available in Tab. S3

At the end of BD, total VLA_{emb} was about 0.4 mm mm^{-2} for all the species. For Oc, VLA_{emb} was similar to VLA_{maj} (Table 2), whereas for Ac and Pn it was higher (Tab. 2), since embolism events were detected also in minor veins. At the end of the GI experiment, VLA_{emb} was about 0.4, 0.6, and 0.8 mm mm^{-2} for Oc, Ac and Pn respectively. For Ac and Pn, higher VLA_{emb} values were detected in the GI vs BD procedure at corresponding absolute pressure values.

Micro-CT observations

High-resolution images were obtained with micro-CT to visualize embolized vessels in the midrib of Pn leaves (Fig. 4). Leaves attached to cut shoots and entire 2-years old plants showed none or very low embolism levels at the -1.10/-1.20 MPa Ψ range, consistent with the BD-based OVc. The entire xylem area in the midrib of both leaves attached to cut shoots and entire plants was embolized at -1.60/-1.70 MPa Ψ values, i.e. within P_{50} CIs in the GI

For Peer Review

procedure (Tab. 1) and corresponding to Ψ values triggering the propagation of emboli in the BD procedure (Fig. 1).

DISCUSSION

Both BD and GI procedures induced embolism formation in the leaf vein network of the three studied species, allowing us to construct optical vulnerability curves for calculation of species- and method-specific P_{50} values. In both methods, the pattern of embolism formation was similar with early events detected in the major veins. Higher order veins were found to embolize at progressively higher tension (for BD) or gas pressure (for GI). This observation is consistent with several other experiments on leaves of different species based on the optical technique (Brodribb et al. 2016, Hochberg et al. 2019), but at odds with early attempts to visualize the spatial pattern of embolism formation in leaves based on injection of dyes (Salleo et al. 2001, Trifilò et al. 2003). These early studies suggested that embolism was initiated in the minor veins, revealing a possible artefact of such staining techniques related to reduced dye flow to terminal veins following an initial reduction of conductive capacity of major veins, or caused by minor veins collapse and occlusion before embolism occurrence (Zhang et al. 2016). On the other hand, it should be noted that the total VLA_{emb} measured in our study was about 0.5 mm mm^{-2} for the three species, a value higher than VLA_{maj} but significantly lower than VLA_{min}, indicating that any eventual embolism event in the very minor veins could not be detected. Indeed, a direct comparison of total VLA_{emb} with both VLA_{maj} and VLA_{min} is generally not reported in studies using the optical technique, and a visual analysis of published images suggests that in most cases only veins up to 3rd or 4th order can be clearly visualized as embolized (e.g. Brodribb et al. 2016, Creek et al. 2020, Cardoso et al. 2020). This might suggest that minor veins are highly resistant toward embolism formation, or that the optical technique is not always adequate to capture embolism events occurring in the highest order veins.

Despite similar patterns of embolism propagation, the two procedures produced different estimates of leaf vulnerability to xylem embolism. During GI, embolism events were observed at pressures below 1 MPa, in contrast with BD where xylem tension of at least -1 MPa were necessary to induce embolism in Pn, and no embolism event was detected down to -2 MPa in Ac and Oc. As a result. P_{12} values obtained with the GI procedure were significantly higher than those obtained with BD in Oc and Pn (Tab. 1). It should be further noted that GI measurements likely over-estimated the pressure threshold inducing embolism. In fact, the applied pressure was measured at the injection point, but it is likely that resistances interposed between the cut section of the twig and the leaf veins induced a progressive pressure drop (Cochard et al. 2004), making difficult to determine exactly the pressure to which each vein order was actually exposed to during GI. This situation contrasts with the BD procedure, where embolism events generally occur after complete stomatal closure (Creek et al. 2020), so that water potential is expected to substantially equilibrate across the whole leaf and xylem tension is expected to reach the same value in all vein orders during progressive dehydration (Teare and Kanemasu 1972).

The optical vulnerability curves based on BD or GI allowed us to calculate 'optical' P_{12}, P_{50} and P_{88} values. It should be noted that the functional meaning of these metrics remains still debated, because this is essentially based on the measurement of the amount of embolized pixels, which does not necessarily translate into an equivalent reduction of vein water transport capacity (Venturas et al. 2019), due to the typical redundancy of the vein network (Scoffoni and Jansen 2016) and complexity of the water transport pathways in the leaf (Salleo et al. 2003). On the other hand, other studies found good agreement between optical and hydraulic P_{50} values, both at stem (Gauthey et al. 2020; Avila et al. 2023) and leaf (Brodribb et al. 2016) level. Regardless of its exact functional meaning, P_{12} and P_{50} of our study species were significantly different when estimated on the basis of BD or GI. Considering P_{50}, the vulnerability to xylem embolism was overestimated by only 0.19 MPa in Ac, but by as much as 0.43 and 0.57 MPa in Oc and Pn. This trend apparently reflects the species-specific vessel lengths, which were lowest in Ac and progressively higher in Oc and Pn. Similarly, Hochberg

For Peer Review

et al. (2019) reported higher P_{50} values obtained with GI vs BD procedures in *V. vinifera* (ΔP_{50} = 0.40 MPa), which has a vessel length close to Pn (Zimmermann and Jeje, 1981; Venturas et al. 2016).

In our analysis, VLA_{emb} was used as a measurement of optical embolism, as suggested in Petruzzellis et al. (2020), while previous studies quantified optical embolism by calculating the percentage of embolized xylem area (Brodribb et al. 2016; Cardoso et al. 2020; Avila et al. 2021). As mentioned above, measuring VLA_{emb} allowed us to measure OV curves and Ψ_{leaf} on the same leaves, while the above studies used adjacent leaves, assuming that they have the same embolization pattern during leaf dehydration. Despite reducing the variability due to the choice of different leaves, the VLA_{emb} approach could overweight the embolism events occurring in minor order veins, which contribute minimally to the leaf xylem hydraulic conductance. This could potentially lead to artificially low 'optical' P_{12}, P_{50} and P_{88} values. Our analysis suggests that VLA_{emb} underestimate P_{88} values (Tab. S2) if compared to the % of embolized area (Tab. S2), while similar values were obtained for P_{12} and P_{50} in two out of three species (except for Pn) using the two different approaches. These results overall support the hypothesis that the GI method applied to leaf optical vulnerability curves could be affected by the 'open-vessel' artefact, which is well known as a source of error in other hydraulic and imaging techniques aimed at quantifying xylem vulnerability to embolism formation (Martin-StPaul et al. 2014, Torres-Ruiz et al. 2014; Guan et al. 2021).

Furthermore, the open-vessel artefact might also affect the OVc based on BD of cut branches, like actually done in our experiments. To check for this possible additional source of error, we performed micro-CT observations of both cut shoots and intact plants of Pn dehydrated to different target water potential values. In the case of cut shoots, the leaf midrib showed none or very few embolized conduits at a water potential of about -1.2 MPa, consistent with the OVc obtained with the BD procedure but again at odds with that derived on the basis of GI. Upon water potential drop to about -1.6 MPa, most xylem conduits appeared embolized in the midrib of leaves from both entire plants and cut shoots, in accordance to the OVc obtained with both procedures, which showed VLA_{emb} values close to 0.1 mm mm^{-2} (ca. 30% of

For Peer Review

maximum VLA_{emb}) and 0.4 mm mm^{-2} (ca 50% of maximum VLA_{emb}) for BD and GI, respectively. These observations further confirm that the GI method largely overestimated the vulnerability to xylem embolism of the leaf vein network.

It should be considered that our GI experiments were performed using dry compressed N_2, and it is possible that pit membrane dehydration caused by the treatment also contributed to increased vulnerability to embolism compared to bench dehydration. It would be interesting to test in future studies whether the use of humidified air might improve the reliability of OVc based on gas injection.

Overall, our data indicate that GI is not a reliable technique for quantification of leaf hydraulic vulnerability, suggesting that accurate detection of xylem embolism in the leaf vein network should be preferably based on BD of intact up-rooted plants. Unfortunately, these findings also imply that we still do not have any 'fast' and reliable technique to quantify the P_{50} of leaves of different species, somehow limiting the possibilities to currently include this important functional trait in broad-scale studies or for agronomic purposes.

CONFLIC OF INTEREST

None declared.

DATA AVAILABILITY

The data that support the findings of this study are available from the corresponding author, FP, upon reasonable request.

FUNDING

The study was supported by the University of Trieste (Finanziamenti per la Ricerca di Ateneo 2018 – Project WatPlantClim:Plant water relations and hydraulic traits for mechanistic modelling of the impact of climate change on plant distribution) and by the Interreg V-A Italia-Slovenija programme 2014–2020 (Project SECAP: Supporting energy and climate adaptation policies). FP is currently supported by the funding PON Ricerca e Innovazione D.M. 1062/21–

For Peer Review

Contratti di ricerca, from the Italian Ministry of University (MUR). ET is currently supported by Estonian Research Council (grant code MOBJD1030).

AUTHORS' CONTRIBUTION

FP, ADB, ET, GB and AN designed and planned the experiments; FP, ADB, ET, PT and AN designed the experimental set up and performed the experimental measurements. FP, MT, SN, GT, FDL, LA and AN performed micro-CT observation. FP, ET, GB and AN analysed data. FP and AN wrote the manuscript, with contribution from all co-authors.

For Peer Review

REFERENCES

Alvarez-Cansino L, Comita LS, Jones FA, Manzané-Pinzòn E, Browne L, Engelbrecht BMJ (2022) Turgor loss point predicts survival responses to experimental and natural drought in tropical tree seedlings. Ecology 103:e3700.

Avila RT, Kane CN, Batz TA, Trabi C, Damata FM, Jansen S, McAdam SAM (2023). The relative area of vessels in xylem correlates with stem embolism resistance within and between genera. Tree Physiol 43: 75-87.

Avila RT, Cardoso AA, Batz TA, Kane CN, DaMatta FM, McAdam SAM (2021) Limited plasticity in embolism resistance in response to light in leaves and stems in species with considerable vulnerability segmentation. Physiol Plant 172, 2142–2152.

Bartlett MK, Scoffoni C, Sack L (2012) The determinants of leaf turgor loss point and prediction of drought tolerance of species and biomes: a global meta-analysis. Ecol Lett 15:393-405.

Blackman CJ (2018) Leaf turgor loss as a predictor of plant drought response strategies. Tree Physiol 38:655-657.

Blackman CJ, Li X, Choat B, Rymer PD, De Kauwe MG, Duursma RA, Tissue DT, Medlyn BE (2019) Desiccation time during drought is highly predictable across species of *Eucalyptus* from contrasting climates. New Phytol 224:632-643.

Brodribb TJ, Skelton RP, McAdam SAM, Bienaimé D, Lucani CJ, Marmottant P (2016) Visual quantification of embolism reveals leaf vulnerability to hydraulic failure. New Phytol 209:1403-1409.

Brun F, Pacile S, Accardo A, Kourousias G, Dreossi D, Mancini L, Tromba G, Pugliese R (2015) Enhanced and flexible software tools for X-ray computed tomography at the Italian synchrotron radiation facility Elettra. Fundam Inform 141:233-243.

For Peer Review

Bucci SJ, Carbonell Silletta LM, Garré A, Cavallaro A, Thais Efron ST, Arias NS, Goldstein G, Scholz FG (2019) Functional relationships between hydraulic traits and the timing of diurnal depression of photosynthesis. Plant Cell Environ 42:1603-1614.

Bühler J, Rishmawi L, Pflugfelder D, Huber G, Scharr H, Hülskamp M, Koornneef M, Schurr U, Jahnke S (2015) phenoVein - A tool for leaf vein segmentation and analysis. Plant Physiol 169:2359-2370.

Cardoso AA, Batz TA, McAdam SAM (2020) Xylem embolism resistance determines leaf mortality during drought in *Persea americana*. Plant Physiol 182:547-554.

Cardoso AA, Kane CN, Rimer IM, McAdam SAM (2022) Seeing is believing: what visualising bubbles in the xylem has revealed about plant hydraulic function. Funct Plant Biol 49:759-772.

Chen YJ, Maenpuen P, Zhang YJ, Barai K, Katabuchi M, Gao H, Kaewkamol S, Tao LB, Zhang JL (2021) Quantifying vulnerability to embolism in tropical trees and lianas using five methods: can discrepancies be explained by xylem structural traits? New Phytol 229:805-819.

Choat B, Ball M, Luly J, Holtum J (2003) Pit membrane porosity and water stress-induced cavitation in four co-existing dry rainforest tree species. Plant Physiol 131:41-48.

Cochard H, Cruiziat P, Tyree MT (1992) Use of positive pressures to establish vulnerability curves - Further support for the air-seeding hypothesis and implications for pressure-volume analysis. Plant Physiol 100:205-209.

Cochard H, Nardini A, Coll L (2004) Hydraulic architecture of leaf blades: where is the main resistance? Plant Cell Environ 27:1257-1267.

Cosme LHM, Schietti J, Costa FRC, Oliveira RS (2017) The importance of hydraulic architecture to the distribution patterns of trees in a central Amazonian forest. New Phytol 215:113-125.

For Peer Review

Creek D, Lamarque LJ, Torres-Ruiz JM, Parise C, Burlett R, Tissue DT, Delzon S (2015) Xylem embolism in leaves does not occur with open stomata: evidence from direct observations using the optical visualization technique. J Exp Bot 71:1151-1159.

Duursma RA, Choat B (2017) fitplc - an R package to fit hydraulic vulnerability curves. J Plant Hydr 4:e-002.

Ennajeh M, Simões F, Khemira H, Cochard H (2011a) How reliable is the double-ended pressure sleeve technique for assessing xylem vulnerability to cavitation in woody angiosperms? Physiol Plant 142:205-210.

Ennajeh M, Nouiri M, Khemira H, Cochard H (2011b) Improvement to the air-injection technique to estimate xylem vulnerability to cavitation. Trees 25:705-710.

Fitzgerald R (2000) Phase-sensitive X-ray imaging. Phys Today 53:23–26.

Forzieri G, Dakos V, McDowell NG, Ramdane A, Cescatti A (2022) Emerging signals of declining forest resilience under climate change. Nature 608:534-539.

Gardner WR (1965) Dynamic aspects of soil-water availability to plants. Annu Rev Plant Physiol 16:323-342.

Gauthey A, Peters JMR, Carins-Murphy MR, Rodriguez-Dominguez CM, Li X, Delzon S, King A, López R, Medlyn BE, Tissue DT, Brodribb TJ, Choat B (2020). Visual and hydraulic techniques produce similar estimates of cavitation resistance in woody species. New Phytol 228: 884-897.

Guan X, Pereira L, McAdam SAM, Cao KF, Jansen S (2021) No gas source, no problem: proximity to pre-existing embolism and segmentation affect embolism spreading in angiosperm xylem by gas diffusion. Plant Cell Environ 44:1329–1345.

Hernandez-Santana V, Rodriguez-Dominguez CM, Fernández JE, Diaz-Espejo A (2016) Role of leaf hydraulic conductance in the regulation of stomatal conductance in almond and olive in response to water stress. Tree Physiol 36:725-735.

For Peer Review

Hochberg U, Ponomarenko A, Zhang YJ, Rockwell FE, Holbrook NM (2019) Visualizing embolism propagation in gas-injected leaves. Plant Physiol 180:874-881.

Kavanagh KL, Bond BJ, Aitken SN, Gartner BL, Knowe S (1999) Shoot and root vulnerability to xylem cavitation in four populations of Douglas-fir seedlings. Tree Physiol 19:31-37.

Kunert N, Zailaa J, Herrmann V, Muller-Landau HC, Wright SJ, Pérez R, McMahon SM, Condit RC, Hubbell SP, Sack L, Davies SJ, Anderson-Teixeira KJ (2021) Leaf turgor loss point shapes local and regional distributions of evergreen but not deciduous tropical trees. New Phytol 230:485-496.

Lenz TI, Wright IJ, Westoby M (2006) Interrelations among pressure-volume curve traits across species and water availability gradients. Physiol Plant 127:423-433.

Levionnois S, Kaack L, Heuret P, Abel N, Ziegler C, Coste S, Stahl C, Jansen S (2022) Pit characters determine drought-induced embolism resistance of leaf xylem across 18 Neotropical tree species. Plant Physiol 190:371-386.

Lobell DB, Gourdji SM (2012) The influence of climate change on global crop productivity. Plant Physiol 160:1686-1697.

Maherali H, DeLucia EH (2000) Xylem conductivity and vulnerability to cavitation of ponderosa pine growing in contrasting climates. Tree Physiol 20:859-867.

Maréchaux I, Bartlett MK, Sack L, Baraloto C, Engel J, Joetzjer E, Chave J (2015) Drought tolerance as predicted by leaf water potential at turgor loss point varies strongly across species within an Amazonian forest. Funct Ecol 29:1268-1277.

Martin-StPaul NK, Longepierre D, Huc R, Delzon S, Burlett R, Joffre R, Rambal S, Cochard H (2014) How reliable are methods to assess xylem vulnerability to cavitation? The issue of 'open vessel' artifact in oaks. Tree Physiol 34:894-905.

McDowell NG, Sapes G, Pivovaroff A, Adams HD, Allen CD, Anderegg WRL, Arend M, Breshears DD, Brodribb T, Choat B, Cochard H, De Cáceres M, De Kauwe MG, Grossiord C, Hammond WM, Hartmann H, Hoch G, Kahmen A, Klein T, Mackay DS, Mantova M,

For Peer Review

576 Martínez-Vilalta J, Medlyn BE, Mencuccini M, Nardini A, Oliveira RS, Sala A, Tissue DT,
577 Torres-Ruiz JM, Trowbridge AM, Trugman AT, Wiley E, Xu C (2022) Mechanisms of woody-
578 plant mortality under rising drought, CO2 and vapour pressure deficit. Nature Rev Earth
579 Environ 3:294-308.

580 Nardini A, Battistuzzo M, Savi T (2013) Shoot desiccation and hydraulic failure in temperate
581 woody angiosperms during an extreme summer drought. New Phytol 200:322-329.

582 Nardini A, Õunapuu-Pikas E, Savi T (2014) When smaller is better: leaf hydraulic
583 conductance and drought vulnerability correlate to leaf size and venation density across four
584 *Coffea arabica* genotypes. Funct Plant Biol 41:972-982.

585 Nardini A, Luglio J (2014) Leaf hydraulic capacity and drought vulnerability: possible trade-
586 offs and correlations with climate across three major biomes. Funct Ecol 28:810-818.

587 Nardini A, Pedà G, La Rocca N (2012). Trade-offs between leaf hydraulic capacity and
588 drought vulnerability: morpho-anatomical bases, carbon costs and ecological consequences.
589 New Phytol 196:788-798.

590 Nardini A, Salleo S (2003) Effects of the experimental blockage of the major veins on
591 hydraulics and gas exchange of *Prunus laurocerasus* L. leaves. J Exp Bot 54:1213-1219.

592 Nardini A, Tyree MT, Salleo S (2001) Xylem cavitation in the leaf of *Prunus laurocerasus* and
593 its impact on leaf hydraulics. Plant Physiol 125:1700-1709.

594 Neufeld HS, Grantz DA, Meinzer FC, Goldstein G, Crisosto GM, Crisosto C (1992) Genotypic
595 variability in vulnerability of leaf xylem to cavitation in water-stressed and well-Irrigated
596 sugarcane. Plant Physiol 100:1020-1028.

597 Ogle K, Barber JJ, Willson C, Thompson B (2009) Hierarchical statistical modeling of xylem
598 vulnerability to cavitation. New Phytol 182: 541–554.

599 Oliveira RS, Costa FRC, van Baalen E, de Jonge A, Bittencourt PR, Almanza Y, Barros FV,
600 Cordoba EC, Fagundes MV, Garcia S, Guimaraes ZTM, Hertel M, Schietti J, Rodrigues-

For Peer Review

Souza J, Poorter L (2019) Embolism resistance drives the distribution of Amazonian rainforest tree species along hydro-topographic gradients. New Phytol 221:1457-1465.

Petruzzellis F, Savi T, Bacaro G, Nardini A (2019) A simplified framework for fast and reliable measurement of leaf turgor loss point. Plant Physiol Biochem 139:395-399.

Petruzzellis F, Tomasella M, Miotto A, Natale S, Trifilò P, Nardini A (2020) A leaf selfie: using a smartphone to quantify leaf vulnerability to hydraulic dysfunction. Plants 9:234.

Petruzzellis F, Tordoni E, Tomasella M, Savi T, Tonet V, Palandrani C, Castello M, Nardini A, Bacaro G (2021) Functional differentiation of invasive and native plants along a leaf efficiency/safety trade-off. Env Exp Bot 188:104518.

Petruzzellis F, Tordoni E, Di Bonaventura A, Tomasella M, Natale S, Panepinto F, Bacaro G, Nardini A (2022) Turgor loss point and vulnerability to xylem embolism predict species-specific risk of drought-induced decline of urban trees. Plant Biol 24:1198-1207.

Pockman WT, Sperry JS (2000) Vulnerability to xylem cavitation and the distribution of Sonoran desert vegetation. Am J Bot 87:1287-1299.

Rodriguez-Dominguez CM, Buckley TN, Egea G, de Cires A, Hernandez-Santana V, Martorell S, Diaz-Espejo A (2016) Most stomatal closure in woody species under moderate drought can be explained by stomatal responses to leaf turgor. Plant Cell Environ 39:2014-2026.

Sack L, Holbrook NM (2006) Leaf hydraulics. Annu Rev Plant Biol 57:361-381.

Salleo S, Hinckley TM, Kikuta SB, Lo Gullo MA, Weilgony P, Yoon TM, Richter H (1992) A method for inducing xylem emboli in situ: experiments with a field-grown tree. Plant Cell Environ 15:491-497.

Salleo S, Lo Gullo MA, Raimondo F, Nardini A (2001) Vulnerability to cavitation of leaf minor veins: any impact on leaf gas exchange? Plant Cell Environ 24:851-859.

For Peer Review

Salleo S, Raimondo F, Trifilò P, Nardini A (2003) Axial-to-radial water permeability of leaf major veins: a possible determinant of the impact of vein embolism on leaf hydraulics? Plant Cell Environ 26:1749-1758.

Schneider CA, Rasband WS, Eliceiri KW (2012) NIH Image to ImageJ: 25 years of image analysis. Nat Methods 9: 671–675.

Scoffoni C, Jansen S (2016) I can see clearly now – embolisms in leaf veins. Trends Plant Sci 21:723-725.

Skelton RP (2019) Injecting new life into a classic technique. Plant Physiol 180:706-707.

Skelton RP, Dawson TE, Thompson SE, Shen Y, Weitz AP, Ackerly D (2018) Low vulnerability to xylem embolism in leaves and stems of North American oaks. Plant Physiol 177:1066-1077.

Slot M, Nardwattanawong T, Hernandez GG, Bueno A, Riederer M, Winter K. (2021) Large differences in leaf cuticle conductance and its temperature response among 24 tropical tree species from across a rainfall gradient. New Phytol 232:1618-1631.

Sperry JS, Ikeda T (1997) Xylem cavitation in roots and stems of Douglas-fir and white fir. Tree Physiol 17:275-280.

Sun Q, Gilgen AK, Signarbieux C, Klaus VH, Buchmann N (2021) Cropping systems alter hydraulic traits of barley but not pea grown in mixture. Plant Cell Environ 44:2912-2924.

Teare ID, Kanemasu ET (1972) Stomatal-diffusion resistance and water potential of soybean and sorghum leaves. New Phytol 71:805-810.

Tordoni E, Petruzzellis F, Nardini A, Savi T, Bacaro G (2019) Make it simpler: alien species decrease functional diversity of coastal plant communities. J Veg Sci 30:498-509.

Tordoni E, Petruzzellis F, Di Bonaventura A, Pavanetto N, Tomasella M, Nardini A, Boscutti F, Martini F, Bacaro G (2022) Projections of leaf turgor loss point shifts under future climate change scenarios. Glob Change Biol 28:6640-6652.

For Peer Review

650 Torres-Ruiz JM, Cochard H, Mayr S, Beikircher B, Diaz-Espejo A, Rodriguez-Dominguez CM,
651 Badel E, Fernández JE (2014) Vulnerability to cavitation in *Olea europaea* current-year
652 shoots: further evidence of an open-vessel artefact associated with centrifuge and air-
653 injection techniques. Physiol Plant 152:465-474.

654 Trifilò P, Nardini A, Lo Gullo MA, Salleo S (2003) Vein cavitation and stomatal behaviour of
655 sunflower (*Helianthus annuus*) leaves under water limitation. Physiol Plant 119:409-417.

656 Trifilò P, Raimondo F, Lo Gullo MA, Barbera PM, Salleo S, Nardini A (2014) Relax and refill:
657 xylem rehydration prior to hydraulic measurements favours embolism repair in stems and
658 generates artificially low PLC values. Plant Cell Environ 37:2491-2499.

659 Tyree MT, Ewers FW (1991) The hydraulic architecture of trees and other woody plants. New
660 Phytol 119:345-360.

661 Tyree MT, Hammel HT (1972) The measurement of the turgor pressure and the water
662 relations of plants by the pressure-bomb technique. J Exp Bot 23:267-282.

663 Tyree MT, Sperry JS (1989) Vulnerability of xylem to cavitation and embolism. Annu Rev
664 Plant Physiol 40:19-38.

665 Venturas MD, Pratt RB, Jacobsen AL, Castro V, Fickle JC, Hacke UG (2019) Direct
666 comparison of four methods to construct xylem vulnerability curves: differences among
667 techniques are linked to vessel network characteristics. Plant Cell Environ 42:2422-2436.

668 Venturas MD, Sperry JS, Hacke UG (2017) Plant xylem hydraulics: What we understand,
669 current research, and future challenges. J Integr Plant Biol 59:356-389.

670 Venturas MD, Rodriguez-Zaccaro FD, Pecorella MI, Crous CJ, Jacobsen AL, Pratt RB (2016)
671 Single vessel air injection estimates of xylem resistance to cavitation are affected by vessel
672 network characteristics and sample length. Tree Physiol 36: 1247-1259.

673 Wheeler JK, Huggett BA, Tofte AN, Rockwell FE, Holbrook NM (2013) Cutting xylem under
674 tension or super-saturated with gas can generate PLC and the appearance of rapid recovery
675 from embolism. Plant Cell Environ 36:1938-1949.

For Peer Review

676 Wolfe BT (2020) Bark water vapour conductance is associated with drought performance in
677 tropical trees. Biol Lett 16:20200263.

678 Yan CL, Ni MY, Cao KF, Zhu SD (2020) Leaf hydraulic safety margin and safety-efficiency
679 trade-off across angiosperm woody species. Biol Lett 16:20200456.

680 Zhang YJ, Rockwell FE, Graham AC, Alexander T, Holbrook NM (2016) Reversible leaf xylem
681 collapse: a potential "circuit breaker" against cavitation. Plant Physiol 172:2261-2274.

682 Zhu SD, Chen YJ, Ye Q, He PC, Liu H, Li RH, Fu PL, Jiang GF, Cao KF (2018) Leaf turgor
683 loss point is correlated with drought tolerance and leaf carbon economics traits. Tree Physiol
684 38:658-663.

685 Zimmermann MH, Jeje AA (1981) Vessel-length distribution in stems of some American
686 woody plants. Can J Bot 59: 1882–1892.

687

688

For Peer Review

FIGURE LEGENDS

Fig. 1. Spatial distribution of embolism propagation in leaves of *Acer campestre* (Ac), *Ostrya carpinifolia* (Oc) and *Populus nigra* (Pn) based on bench dehydration (BD) or gas-injection (GI) procedures. Embolism events are coloured according to the corresponding leaf water potential or injection pressure (MPa).

Fig. 2. Optical vulnerability curves measured in *Acer campestre* (Ac), *Ostrya carpinifolia* (Oc) and *Populus nigra* (Pn) based on bench dehydration (BD) or gas injection (GI). The cumulative length of embolized veins per unit area (VLA_{emb}) is showed as a function of leaf water potential (Ψ) or injected pressure (P_{inj}) for BD and GI procedures, respectively. Dashed lines indicate leaf water potential and pressure injected inducing 50% of embolism (P_{50}) (continuous line), while gray and green shaded areas represent 95% confidence intervals P_{50}, as measured with bench dehydration (BD) and gas-injection (GI) procedures, respectively.

Fig. 3. Vessel lengths (cyan colour) and discrepancy between P_{50} values calculated with BD and GI procedures (ΔP_{50}, red colour) in *Acer campestre* (Ac), *Ostrya carpinifolia* (Oc) and *Populus nigra* (Pn).

Fig. 4. Representative transverse sections reconstructed from micro-CT scans, showing the midrib of *Populus nigra* (Pn) leaves attached to intact plants (first row) and cut shoots (second row) at three different Ψ ranges. Dark areas represent gas filled xylem conduits or air spaces.

For Peer Review

712 TABLES

713

714 Table 1. Mean values and associated 95% confidence intervals (CIs) of leaf water potential
715 inducing 12%, 50% and 88% of embolism (P_{12}, P_{50} and P_{88}) measured in *Acer campestre*
716 (Ac), *Ostrya carpinifolia* (Oc) and *Populus nigra* (Pn) with the optical technique, based on
717 bench dehydration (BD) or gas-injection (GI).

718

Species	Dehydration procedure	P_{12} (MPa)	CI 2.5%	CI 97.5%	P_{50} (MPa)	CI 2.5%	CI 97.5%	P_{88} (MPa)	CI 2.5%	CI 97.5%
Ac	BD	-1.73	-1.13	-2.22	-2.87	-2.43	-3.53	-5.74	-4.09	-11.23
	GI	-1.65	-1.40	-1.91	-2.68	-2.46	-2.90	-5.56	-4.12	-6.99
Oc	BD	-1.76	-1.46	-2.12	-2.47	-2.26	-2.67	-4.04	-3.32	-5.51
	GI	-1.10	-0.80	-1.23	-2.04	-1.80	-2.29	-3.90	-2.74	-5.07
Pn	BD	-1.66	-1.52	-1.96	-2.11	-1.98	-2.28	-3.11	-2.10	-4.04
	GI	-0.51	-0.38	-0.64	-1.54	-1.36	-1.72	-2.76	-1.85	-3.66

719

720

For Peer Review

Table 2. Mean values and associated standard deviation of major and minor vein length per unit area (VLA_{maj} and VLA_{min}, respectively) measured in *Acer campestre* (Ac), *Ostrya carpinifolia* (Oc) and *Populus nigra* (Pn).

Species	VLA_{maj} (mm mm^{-2})	VLA_{min} (mm mm^{-2})
Ac	0.25 ± 0.01	9.27 ± 0.60
Oc	0.36 ± 0.03	8.30 ± 0.45
Pn	0.17 ± 0.02	11.93 ± 1.64

For Peer Review

727

Acer campestre

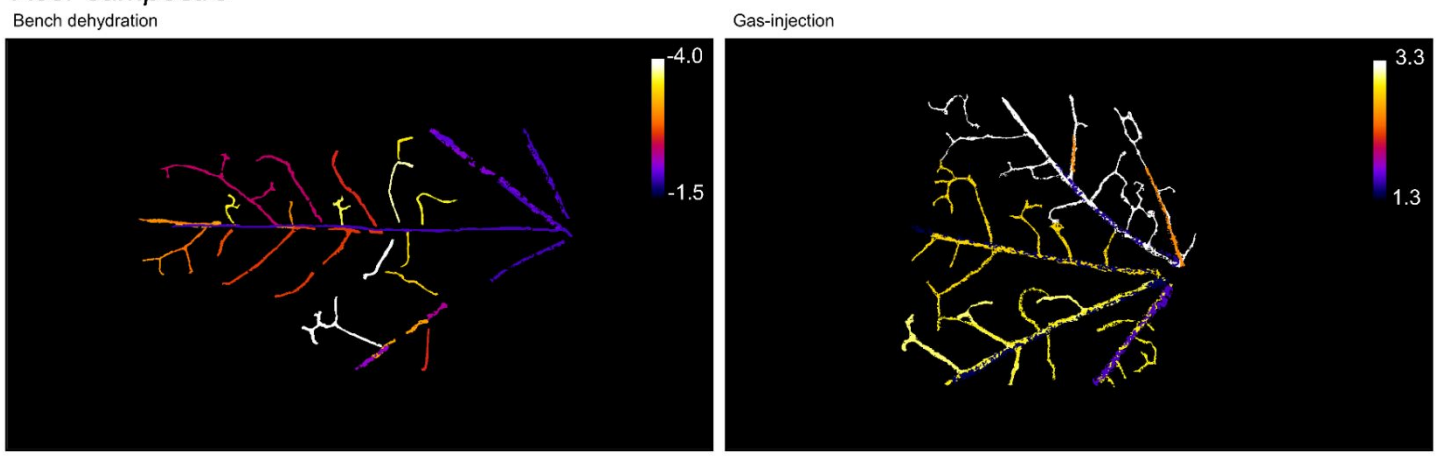

Ostrya carpinifolia

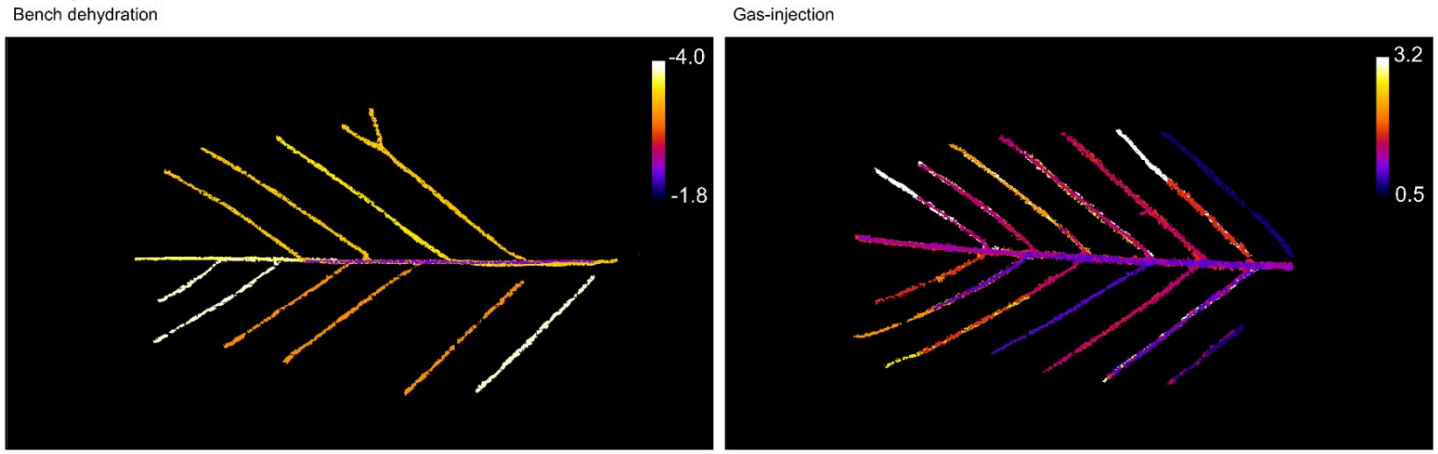

Populus nigra

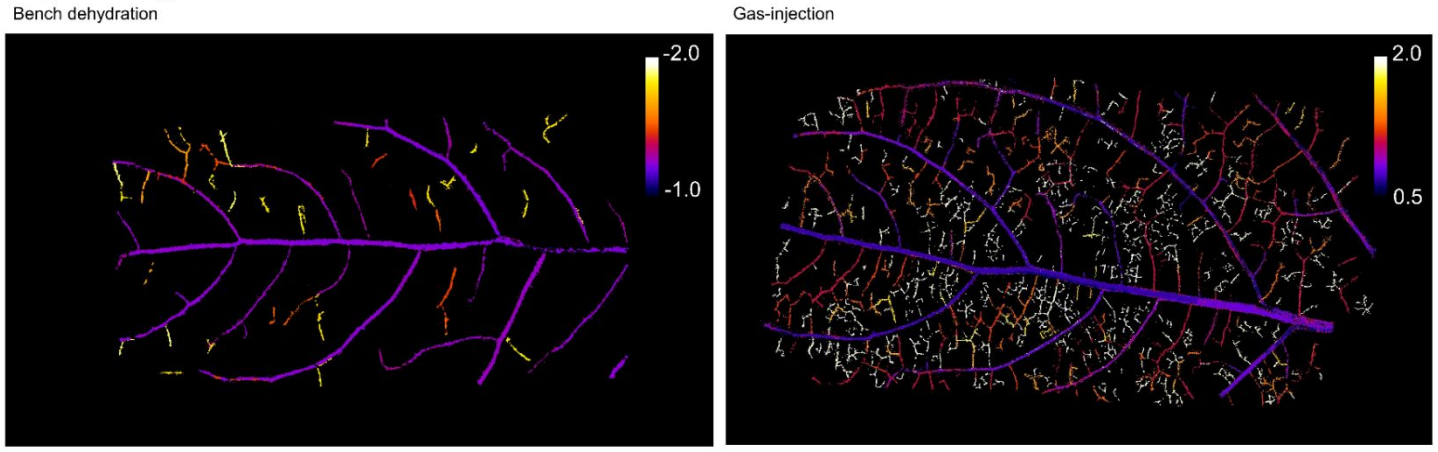

728

729 Figure 1

730

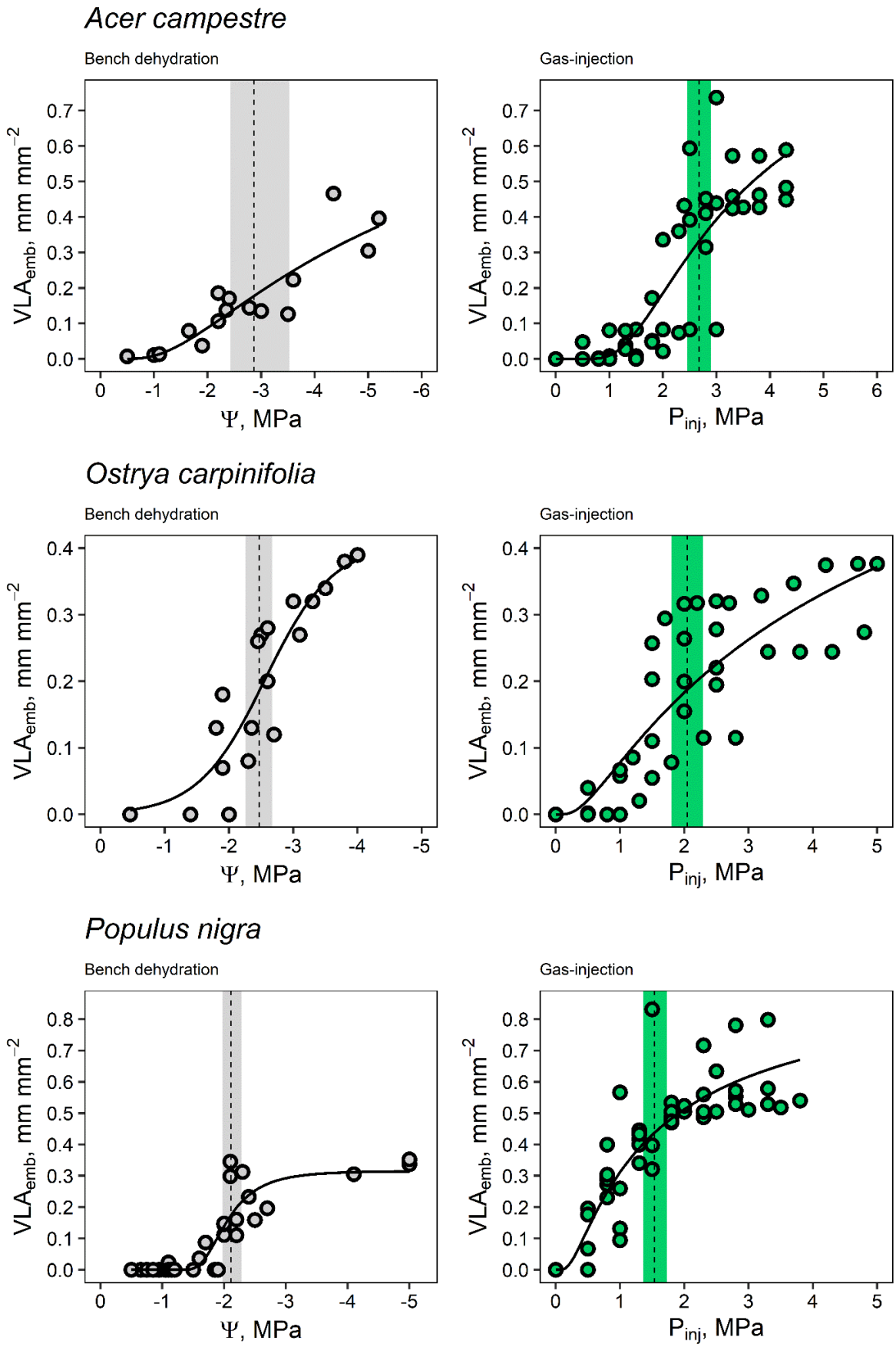

731
732 Figure 2.

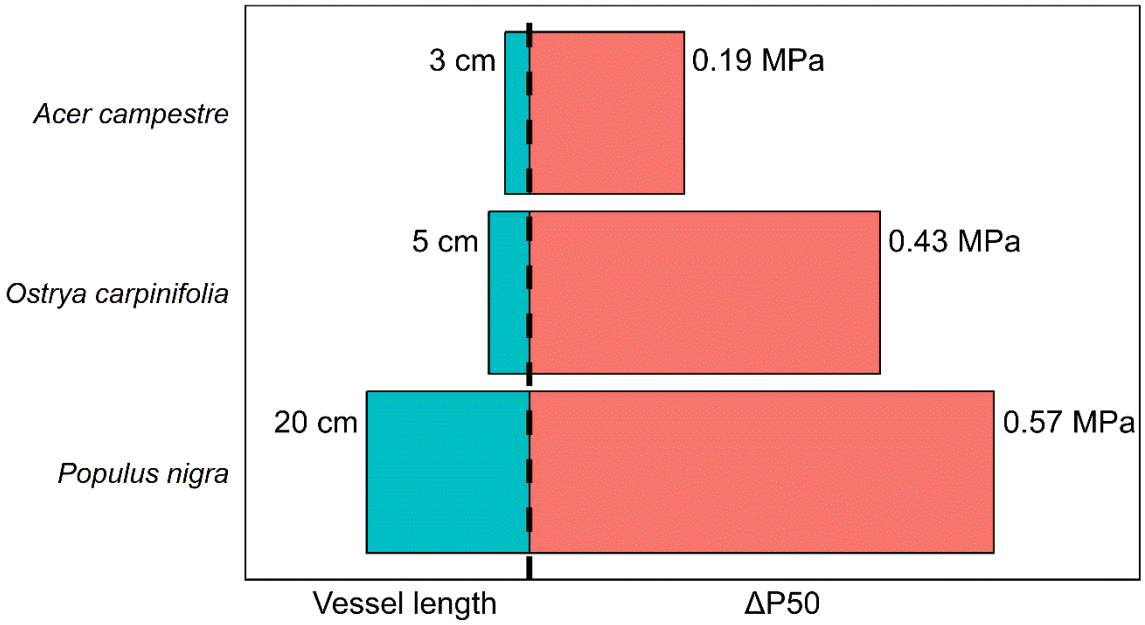

Figure 3.

Peer Review

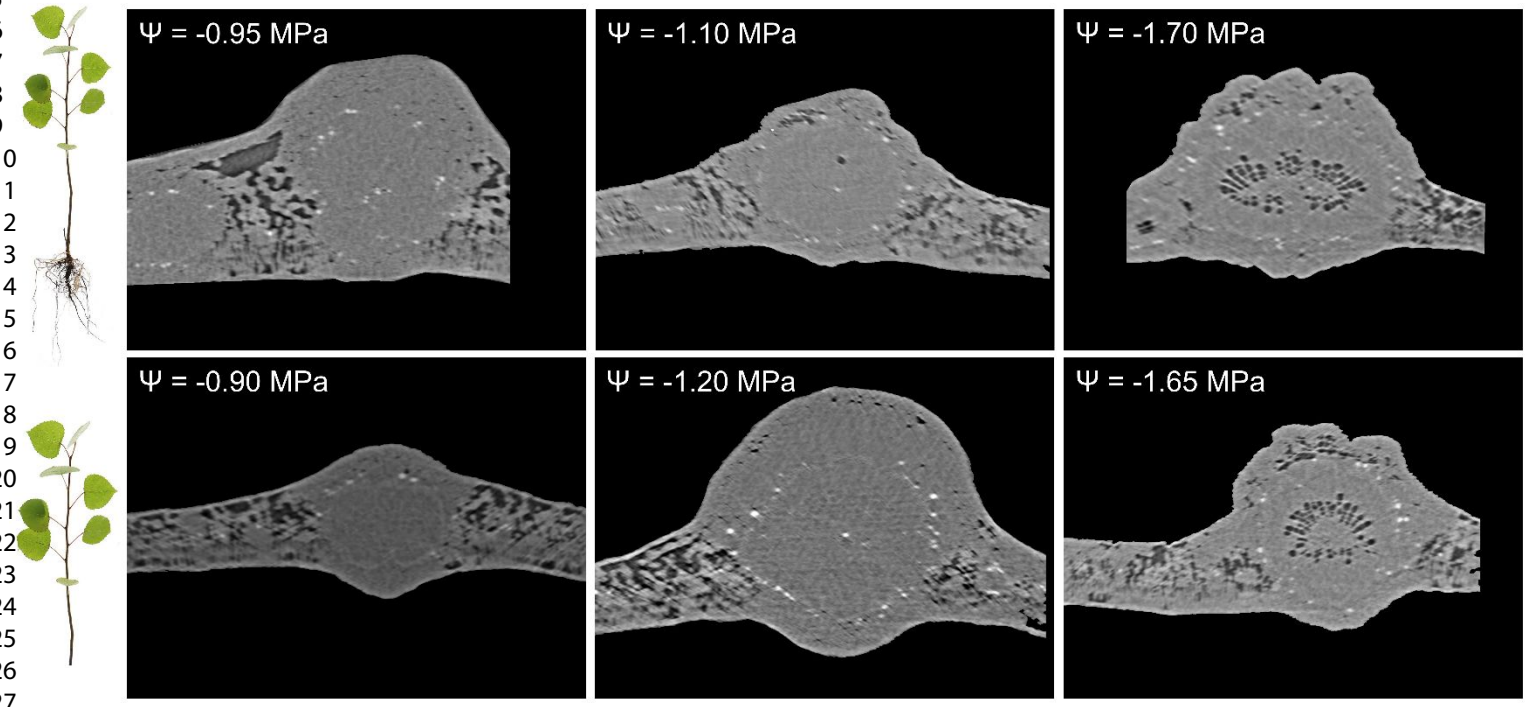

Figure 4.

eer Review